Supplement of
Dynamics of China's tree canopy cover: a China annual tree canopy cover dataset at 30m resolution from 1970s to 2024

Jinge Yu[1], Zhen Yu[1, 2, 3, 4 *], Wangya Han[1, 4], Fangmin Zhang[1, 4], Shirong Liu[2, 3 *]

[1]State Key Laboratory of Climate System Prediction and Risk Management, Nanjing University of Information Science and Technology, Nanjing, 210044, China
[2]Institute of Forestry and Grassland Carbon Sequestration, Chinese Academy of Forestry, Beijing, 100091, China
[3]Key Laboratory of Forest Ecology and Environment, China's National Forestry and Grassland Administration, Ecology and Nature Conservation Institute, Chinese Academy of Forestry, Beijing, 100093, China
[4]Key Laboratory of Ecosystem Carbon Source and Sink, China Meteorological Administration (ECSS-CMA), School of Ecology and Applied Meteorology, Nanjing University of Information Science and Technology, Nanjing, 210044, China

[*]*Correspondence to*: Zhen Yu (zyu@nuist.edu.cn) & Shirong Liu (liusr@caf.ac.cn)

The copyright of individual parts of the supplement might differ from the article licence.

Supplementary

Table (S1–S5)

Table S1. Overview of datasets used for model input variables.

Dataset	Regions	Temporal scope	Spatial resolution	Sources
Landsat	China	1985-2024	30 m	(Cai et al., 2025)
ALCC	China	1985-2022	30 m	(Li et al., 2026)
NASA DEM	Global	2000	30 m	https://www.earthdata.nasa.gov/data/catalog/lpcloud-nasadem-hgt-001
TerraClimate	Global	1985-2024	4638.30 m	(Abatzoglou et al., 2017)

Table S2. Overview of tree canopy cover relate-datasets utilized for comparison.

Dataset	Regions	Temporal scope	Spatial resolution	Sources
MODIS VCF	Global	2000-2020 (Annual)	250 m	https://lpdaac.usgs.gov/products/mod44bv061/
GFCC	Global	2000, 2010, 2015	30 m	(Sexton et al., 2013)
DWTP	Global	2015-2026	10 m	(Brown et al., 2022)
Hansen's GFC	Global	2000	30 m	(Hansen et al., 2013)
CATCD	China	1985-2023	30 m	(Cai et al., 2024)

Table S3. Overview of forest definition datasets used for area comparison.

Dataset	Regions	Temporal scope	Spatial resolution	Sources
Land cover/Land use datasets				
ALCC	China	1985-2022	30 m	(Li et al., 2026)
CLCD	China	1990-2024 (Annual)	30 m	(Yang and Huang, 2021)
GlobeLand30	Global	2000, 2010, 2020	30 m	(Chen et al., 2015)
GLC_FCS30D	Global	1985, 1990, 1995, 2000-2022	30 m	(Zhang et al., 2024)
Datasets Related to tree canopy cover				
MODIS VCF	Global	2000-2020 (Annual)	250 m	https://lpdaac.usgs.gov/products/mod44bv061/
GFCC	Global	2000, 2010, 2015, 2020	30 m	(Sexton et al., 2013)
Hansen's GFC	Global	2000, 2010	30 m	(Hansen et al., 2013)
CATCD	China	1985-2023	30 m	(Cai et al., 2024)

Table. S4. Comparison of candidate models for stand age–stem density relationships across species.

Species	Model	Equation	R^2	Adj_R^2	AIC	p_value
Picea spp.	Exp.	$y = 3248.8 \cdot e^{-0.011x} + 94.7$	0.49	0.49	9398.27	<0.001
	Pow.	$y = 49825.2 \cdot x^{-0.829}$	0.46	0.46	9435.14	<0.001
	Log.	$y = 6260.9 - 1105.055 \cdot \ln(x)$	0.49	0.49	9399.47	<0.001
Larix spp.	Exp.	$y = 6203.4 \cdot e^{-0.024x} + 557.9$	0.59	0.59	11053.82	<0.001
	Pow.	$y = 100000 \cdot x^{-0.964}$	0.60	0.59	11037.45	<0.001
	Log.	$y = 8214.1 - 1508.9 \cdot \ln(x)$	0.56	0.56	11099.35	<0.001
Pinus sylvestris var. *mongolica*	Exp.	$y = 13854.4 \cdot e^{-0.065x} + 387.8$	0.42	0.40	1033.94	<0.001
	Pow.	$y = 100000 \cdot x^{-1.158}$	0.38	0.35	1039.45	<0.001
	Log.	$y = 6254.7 - 1309.52 \cdot \ln(x)$	0.34	0.32	1042.48	<0.001
Pinus tabuliformis	Exp.	$y = 12603.4 \cdot e^{-0.061x} + 606.2$	0.51	0.50	5367.85	<0.001
	Pow.	$y = 100000 \cdot x^{-1.114}$	0.48	0.47	5394.11	<0.001
	Log.	$y = 7250.6 - 1512.494 \cdot \ln(x)$	0.44	0.43	5422.87	<0.001
Pinus armandii	Exp.	$y = 12259 \cdot e^{-0.062x} + 273.9$	0.42	0.39	767.73	<0.001
	Pow.	$y = 100000 \cdot x^{-1.164}$	0.37	0.34	772.85	<0.001
	Log.	$y = 9011 - 2069.26 \cdot \ln(x)$	0.38	0.36	769.59	<0.001
Pinus densata	Exp.	$y = 15000 \cdot e^{-0.059x} + 488.6$	0.53	0.51	1372.16	<0.001
	Pow.	$y = 100000 \cdot x^{-1.1}$	0.46	0.44	1386.82	<0.001
	Log.	$y = 7823.9 - 1634.779 \cdot \ln(x)$	0.43	0.42	1390.18	<0.001
Cupressus funebris	Exp.	$y = 3662.4 \cdot e^{-0.013x} + 338.8$	0.52	0.52	4640.21	<0.001
	Pow.	$y = 44397.5 \cdot x^{-0.773}$	0.51	0.50	4651.27	<0.001
	Log.	$y = 6488.5 - 1096.409 \cdot \ln(x)$	0.51	0.51	4647.26	<0.001
Quercus spp.	Exp.	$y = 8128.2 \cdot e^{-0.032x} + 594.8$	0.58	0.58	17031.05	<0.001
	Pow.	$y = 100000 \cdot x^{-0.983}$	0.57	0.57	17079.91	<0.001
	Log.	$y = 9678 - 1901.524 \cdot \ln(x)$	0.54	0.54	17148.55	<0.001
Betula platyphylla	Exp.	$y = 15000 \cdot e^{-0.057x} + 727.9$	0.44	0.43	8920.93	<0.001
	Pow.	$y = 100000 \cdot x^{-1.054}$	0.39	0.39	8976.24	<0.001
	Log.	$y = 9115.2 - 1893.318 \cdot \ln(x)$	0.36	0.36	9007.11	<0.001

Note: Three candidate models were used to fit the self-thinning process of tree species under similar site conditions. Exp., exponential model; Pow., power model; Log., logarithmic model.

Table S5. Independent test-set validation of plot-scale empirical equations describing stand age–stem density relationships.

Species	Equation	R^2	r	Bias
Picea spp.	$y = 3248.8 \cdot e^{-0.011x} + 94.7$	0.65	0.81	16.94
Larix spp.	$y = 100000 \cdot x^{-0.964}$	0.58	0.80	82.56
Pinus sylvestris var. *mongolica*	$y = 13854.4 \cdot e^{-0.065x} + 387.8$	0.61	0.80	116.73
Pinus tabuliformis	$y = 12603.4 \cdot e^{-0.061x} + 606.2$	0.66	0.82	23.52
Pinus armandii	$y = 12259 \cdot e^{-0.062x} + 273.9$	0.68	0.83	40.71
Pinus densata	$y = 15000 \cdot e^{-0.059x} + 488.6$	0.69	0.84	7.78
Cupressus funebris	$y = 3662.4 \cdot e^{-0.013x} + 338.8$	0.57	0.80	74.66
Quercus spp.	$y = 8128.2 \cdot e^{-0.032x} + 594.8$	0.65	0.81	30.91
Betula platyphylla	$y = 15000 \cdot e^{-0.057x} + 727.9$	0.59	0.77	-4.68

Figure (S1–S8)

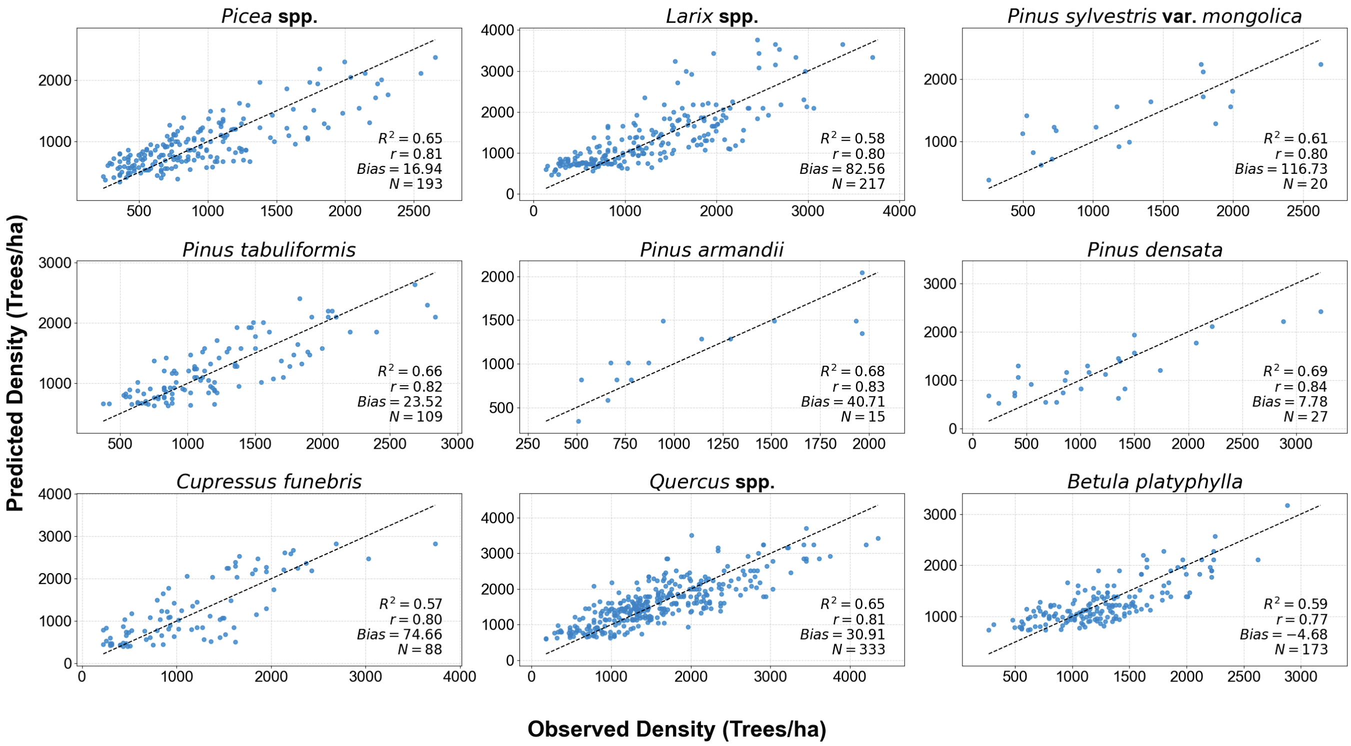

Figure S1. Comparison between observed and predicted stem density for each species.

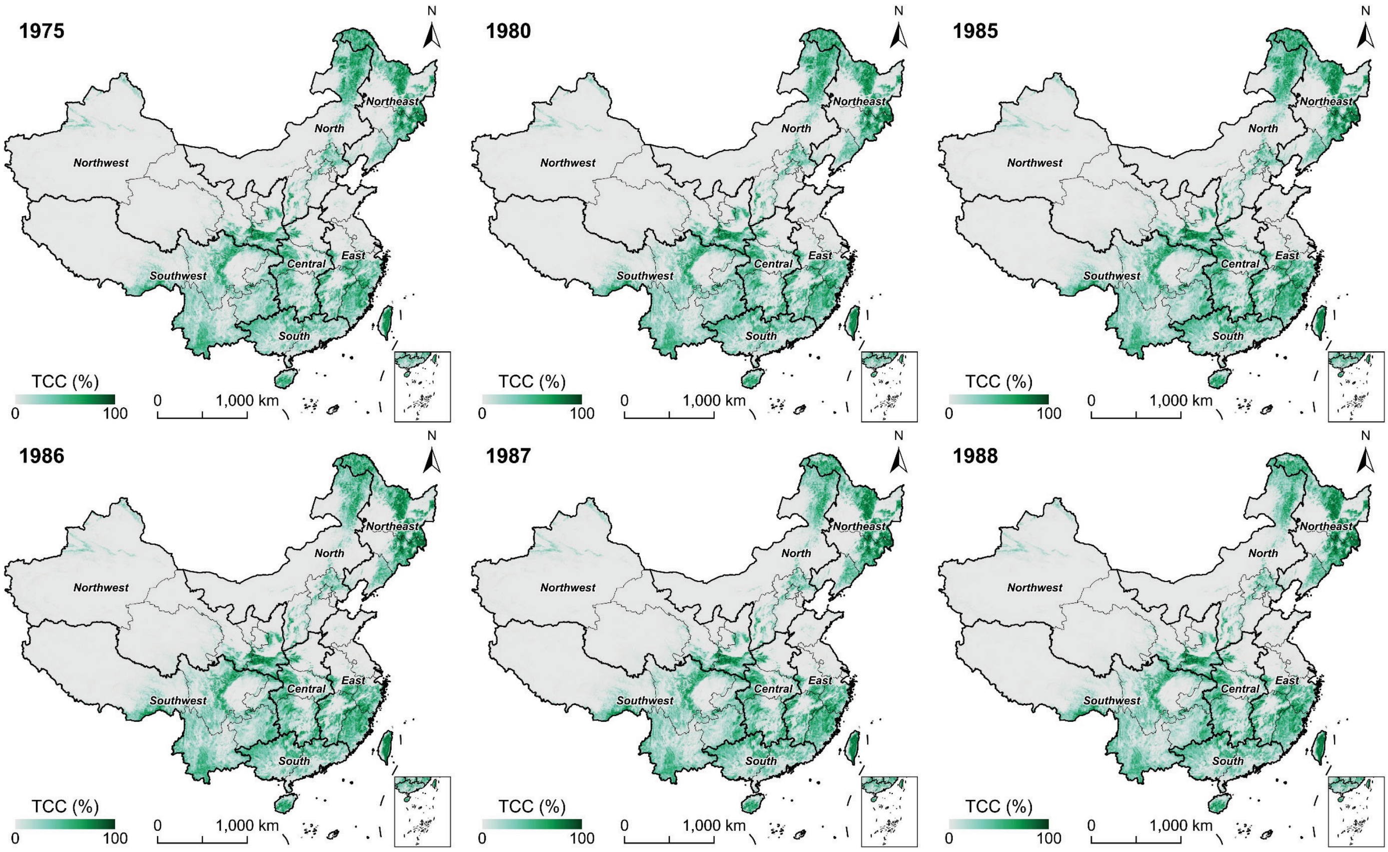

Figure S2. Spatial distribution of ChinaTCC30 in China for 1975, 1980, 1985-1988.

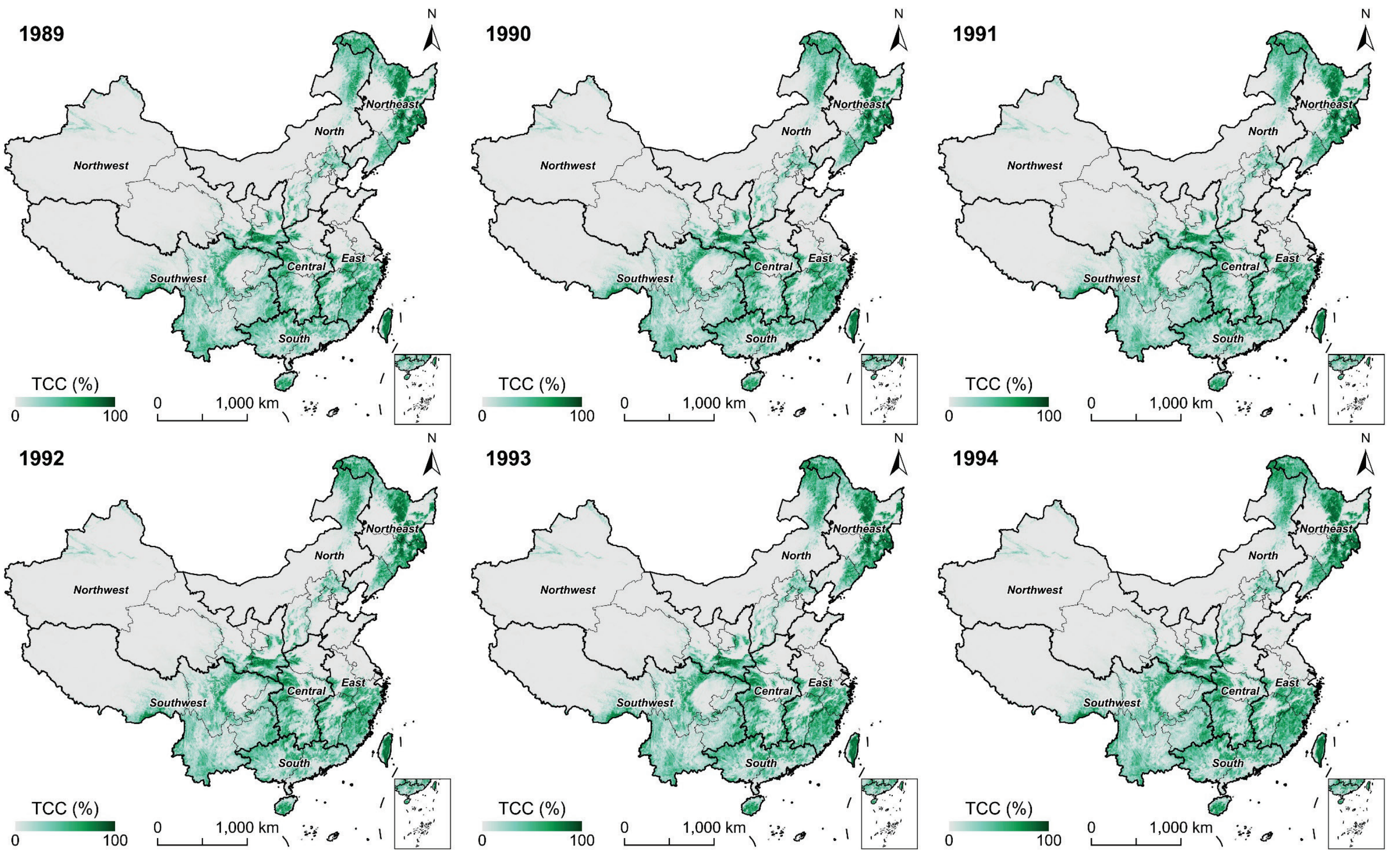

Figure S3. Spatial distribution of ChinaTCC30 in China for 1989-1994.

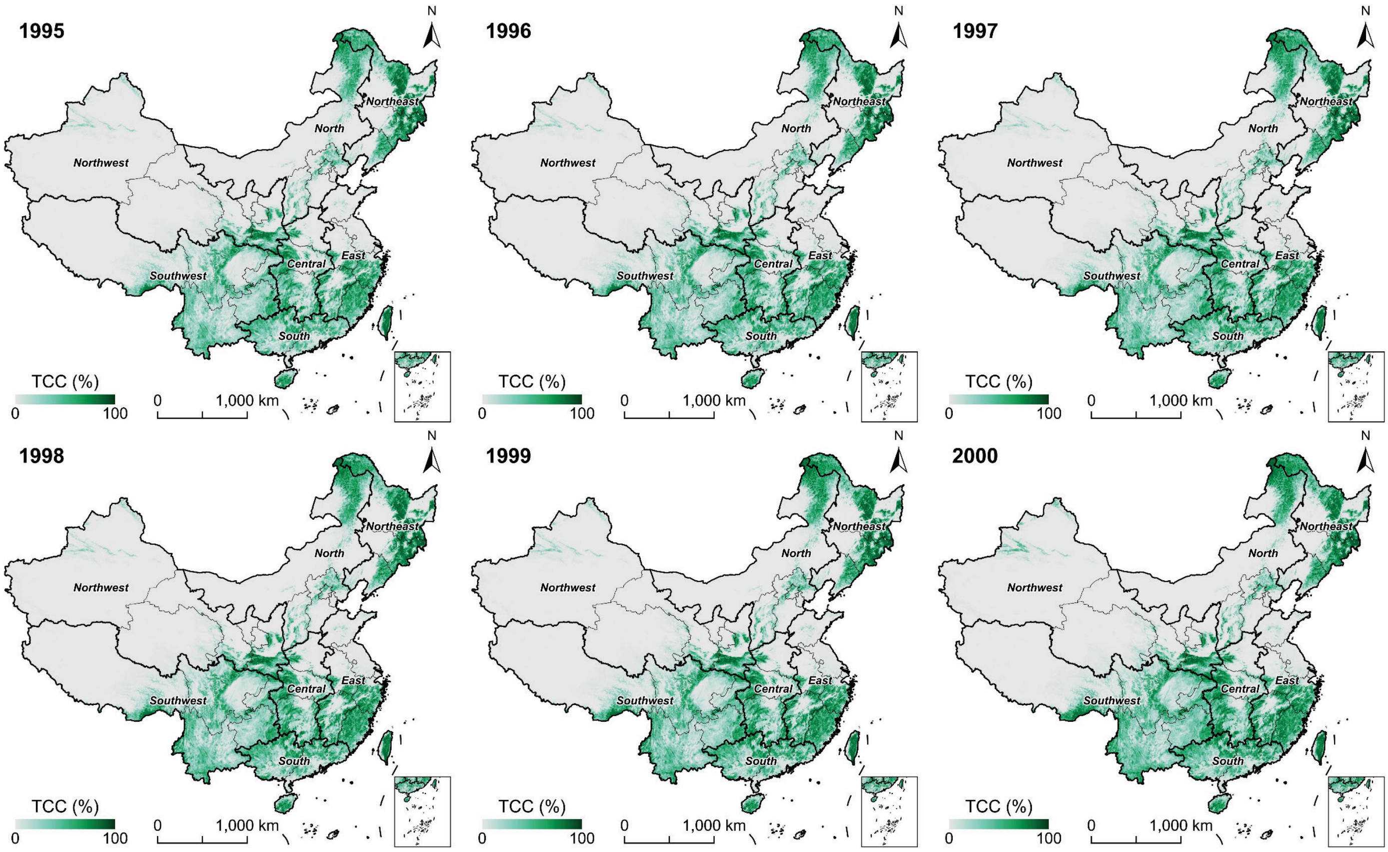

Figure S4. Spatial distribution of ChinaTCC30 in China for 1995-2000.

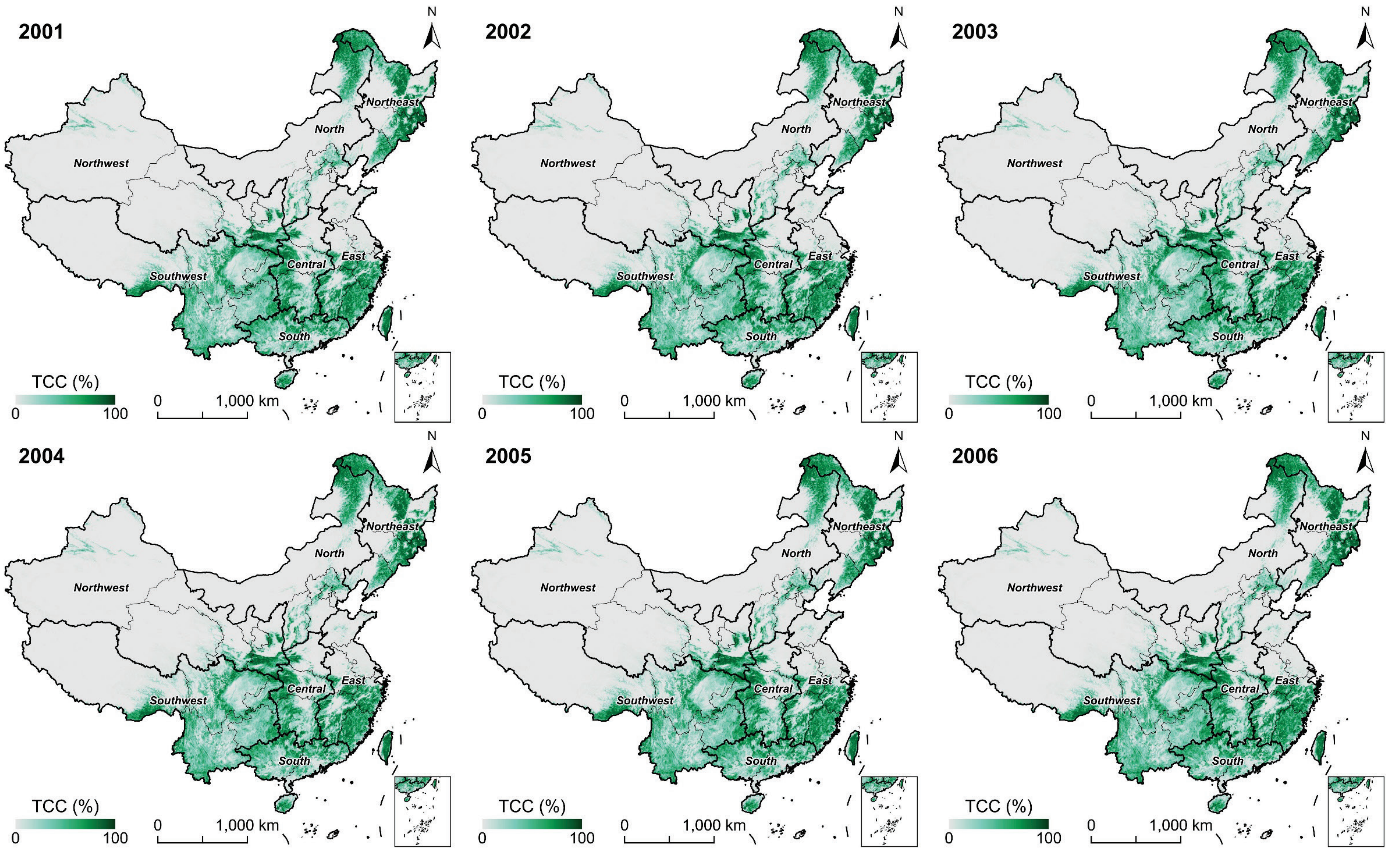

Figure S5. Spatial distribution of ChinaTCC30 in China for 2001-2006.

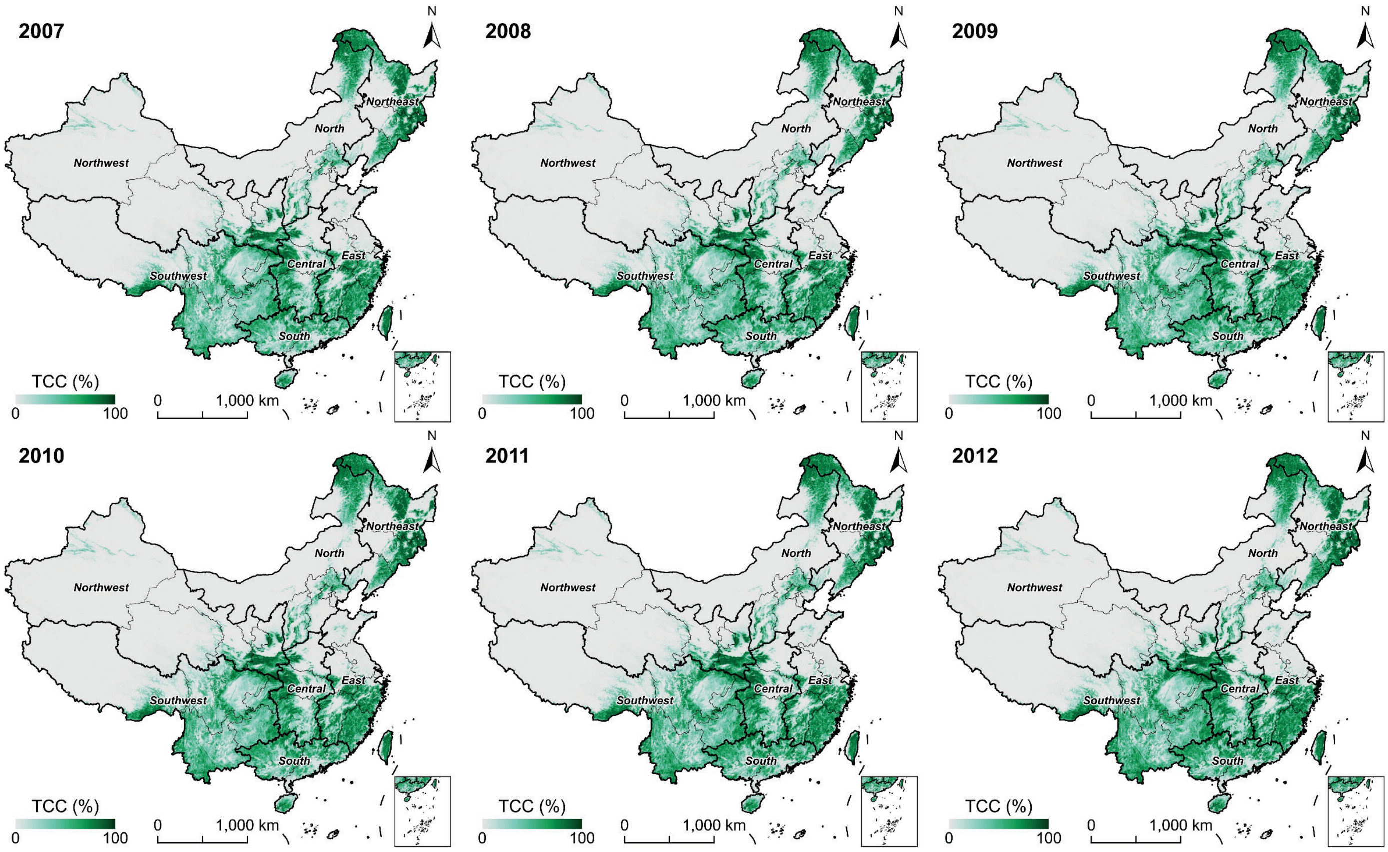

Figure S6. Spatial distribution of ChinaTCC30 in China for 2007-2012.

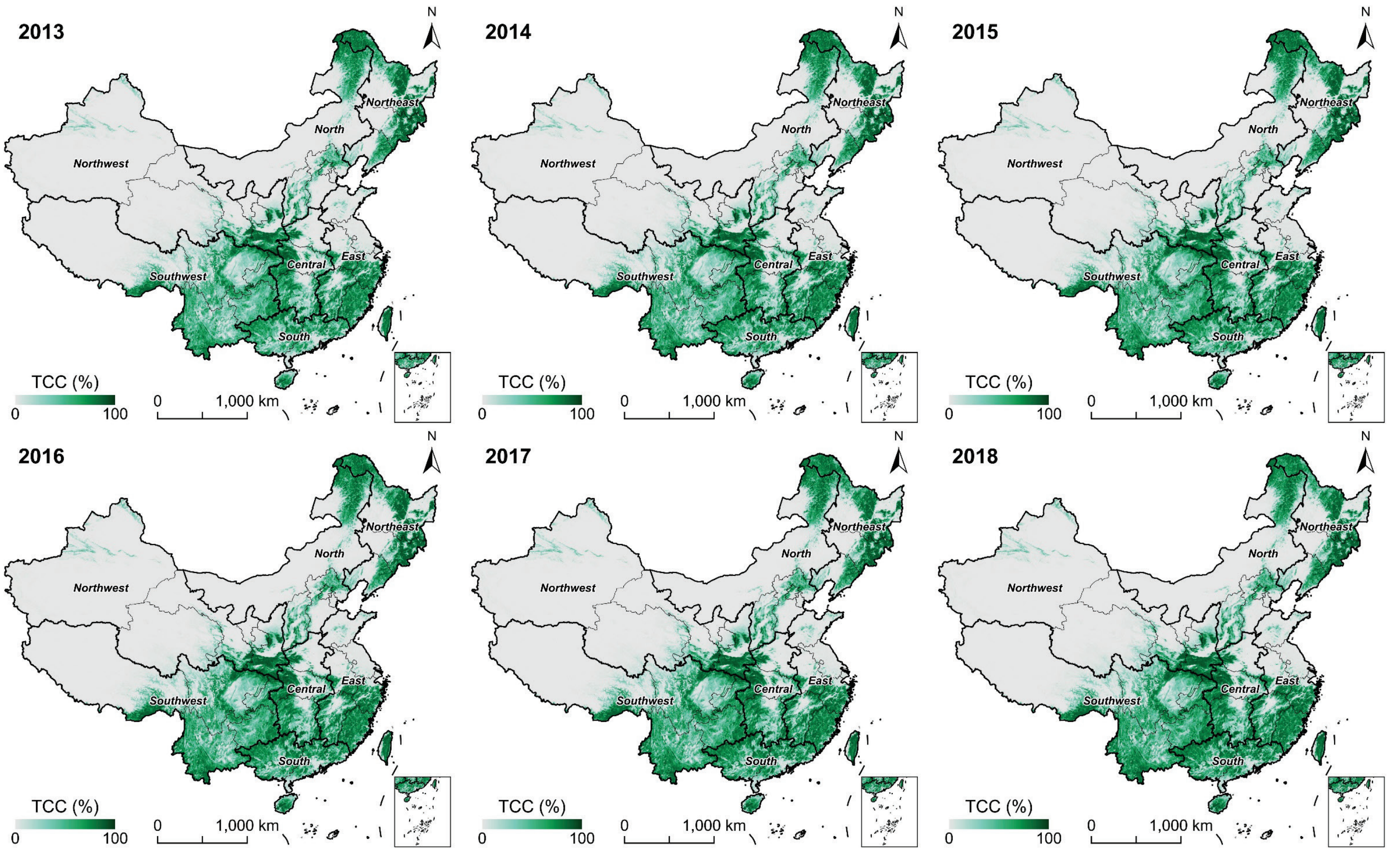

Figure S7. Spatial distribution of ChinaTCC30 in China for 2013-2018.

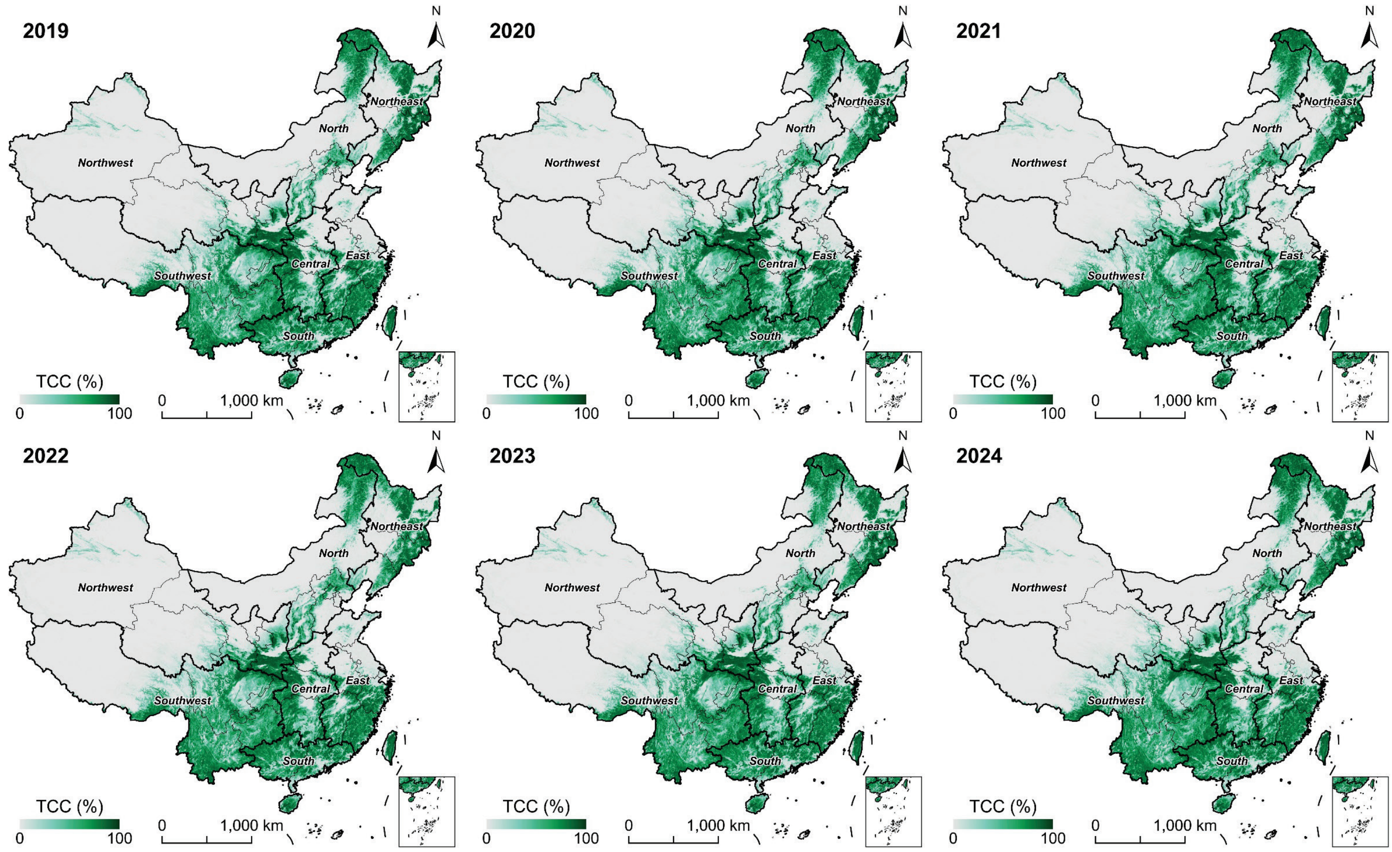

Figure S8. Spatial distribution of ChinaTCC30 in China for 2019-2024.

Bibliography

Abatzoglou, J., Dobrowski, S., Parks, S., and Hegewisch, K.: TerraClimate, a high-resolution global dataset of monthly climate and climatic water balance from 1958–2015. Scientific data. 2018; 5: 170191, 2017.

Brown, C. F., Brumby, S. P., Guzder-Williams, B., Birch, T., Hyde, S. B., Mazzariello, J., Czerwinski, W., Pasquarella, V. J., Haertel, R., and Ilyushchenko, S.: Dynamic World, Near real-time global 10 m land use land cover mapping, Scientific data, 9, 251, https://doi.org/10.1038/s41597-022-01307-4, 2022.

Cai, Y., Li, X., Zhu, P., Nie, S., Wang, C., Liu, X., and Chen, Y.: China Earth Observation Data Cube: The 30-m Seamless Annual Leaf-On Landsat Composites from 1985 to 2023, Journal of Remote Sensing, 5, 0698, 10.34133/remotesensing.0698, 2025.

Cai, Y., Xu, X., Zhu, P., Nie, S., Wang, C., Xiong, Y., and Liu, X.: Unveiling spatiotemporal tree cover patterns in China: The first 30 m annual tree cover mapping from 1985 to 2023, ISPRS Journal of Photogrammetry and Remote Sensing, 216, 240-258, https://doi.org/10.1016/j.isprsjprs.2024.08.001, 2024.

Chen, J., Chen, J., Liao, A., Cao, X., Chen, L., Chen, X., He, C., Han, G., Peng, S., and Lu, M.: Global land cover mapping at 30 m resolution: A POK-based operational approach, ISPRS Journal of Photogrammetry and Remote Sensing, 103, 7-27, https://doi.org/10.1016/j.isprsjprs.2014.09.002, 2015.

Hansen, M. C., Potapov, P. V., Moore, R., Hancher, M., Turubanova, S. A., Tyukavina, A., Thau, D., Stehman, S. V., Goetz, S. J., and Loveland, T. R.: High-resolution global maps of 21st-century forest cover change, science, 342, 850-853, https://doi.org/10.1126/science.1244693, 2013.

Li, B., Liu, X., Zhuang, H., Shi, Q., Zeng, L., Cai, Y., Zhang, H., Cai, Y., Wu, C., and Xu, X.: ALCC: Temporally Consistent Annual Land Cover Maps over China from 1985 to 2022 Based on an Ensemble Change Detection Method, Journal of Remote Sensing, 6, 1029, https://doi.org/10.34133/remotesensing.1029, 2026.

Sexton, J. O., Song, X.-P., Feng, M., Noojipady, P., Anand, A., Huang, C., Kim, D.-H., Collins, K. M., Channan, S., and DiMiceli, C.: Global, 30-m resolution continuous fields of tree cover: Landsat-based rescaling of MODIS vegetation continuous fields with lidar-based estimates of error, International Journal of Digital Earth, 6, 427-448, https://doi.org/10.1080/17538947.2013.786146, 2013.

Yang, J. and Huang, X.: The 30 m annual land cover dataset and its dynamics in China from 1990 to 2019, Earth System Science Data, 13, 3907-3925, 2021.

Zhang, X., Zhao, T., Xu, H., Liu, W., Wang, J., Chen, X., and Liu, L.: GLC_FCS30D: the first global 30 m land-cover dynamics monitoring product with a fine classification system for the period from 1985 to 2022 generated using dense-time-series Landsat imagery and the continuous change-detection method. Earth Syst Sci Data 16 (3): 1353–1381, 2024.